LOW-ENERGY NUCLEAR PHYSICS WITH HIGH-SEGMENTATION SILICON ARRAYS*

R.R. BETTS

Physics Division
Argonne National Laboratory
Argonne, IL 60439, USA
and
Department of Physics
University of Illinois at Chicago
Chicago, IL 60607, USA

(Received December 2, 1994)

A brief history is given of silicon detectors leading up to the development of ion-implanted strip detectors. Two examples of their use in low energy nuclear physics are discussed; the search for exotic alpha-chain states in ^{24}Mg and studies of anomalous positron-electron pairs produced in collisions of very heavy ions.

PACS numbers: 29.40.-n, 25.70.-z

1. Introduction

In this paper, I will first briefly review the historical development of silicon detectors and their application in low-energy nuclear physics. Many new possibilities have recently emerged with the development of surface-passivated ion-implanted silicon detectors, allowing the construction of highly-segmented arrays of detectors, primarily used to date in particle physics applications. Recently, this new type of detector has also been exploited in low-energy nuclear physics. In Section 3, the use of double-sided strip detectors in the study of complex multi-alpha final states produced in low-energy $^{12}C + {}^{12}C$ collisions is described. The application to positron-electron spectroscopy in collisions of very heavy nuclei at Coulomb-barrier energies is presented in Section 4. Future possibilities and challenges are discussed in the concluding section.

---

* Presented at the XXIX Zakopane School of Physics, Zakopane, Poland, September 5–14, 1994.

2. History

The use of solid-state diodes for detection of ionizing particles dates back to the 1950's when the first reports [1] of pulses induced by alpha particles impinging on reverse-biased Ge diodes appeared. The possible beneficial application of such devices to nuclear physics was quite evident due to the increased stopping power of solids and the increased resolution due to the decreased energy required to create an electron-hole pair compared to gases. The first results with Au–Ge junctions were very encouraging, but the need to operate these devices at liquid nitrogen temperature led to attempts to make similar devices with silicon which, due to the larger band gap, were expected to operate near room temperature.

The first practical detectors of this type were made at Chalk River, the junction being formed by evaporation of Au onto the surface of Si — a so-called surface-barrier junction. These devices were used in some pioneering experiments, including some of the very first studies [2] of heavy-ion reactions — $^{12}C + ^{12}C$ scattering, some results of which are shown in Fig. 1.

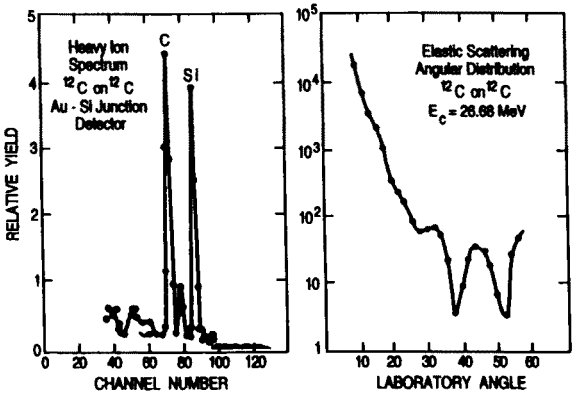

Fig. 1. Spectrum and angular distribution for $^{12}C + ^{12}C$ scattering obtained with an early silicon surface-barrier detector.

Subsequent to these early developments, many different types of diode detectors were developed for nuclear physics applications. Large Ge diodes are used for photon spectroscopy, where the need for resolution supersedes the inconvenience of low-temperature operation. Thick diodes for X-ray and electron spectroscopy have been made using compensated material obtained by drifting Li through the bulk of Si. Surface barrier detectors, although fragile, are commonly used in charged-particle, heavy-ion and fission studies. Position-sensitive detectors are made by forming a resistive layer on the front surface of the diode and obtaining the position information from the charge division between both signal paths in this layer.

Thus, a wide array of detector types are now available which have high resolution and excellent timing properties but suffer from relatively small sizes with which they can be reliably made and ease of damage.

In the 1970's, the discovery of J/psi, a bound state of charmed quark and antiquark, motivated the search for particles with only one charmed quark which were predicted to have lifetimes in the picosecond range and thus decay within only hundreds of microns of their production point. These experiments require high spatial resolution so as to be able to reconstruct decays removed from, but close to, the primary interaction vertex. The need to be able to select events of this type at the trigger level also required fast detectors capable of energy resolution much less than the energy loss of minimum-ionizing particles passing through the detector. These needs were met by junction diodes fabricated using planar technology developed for micro-circuit fabrication.

The steps used in fabrication of silicon detectors by planar processing [3] are shown in Fig. 2. An oxide layer is grown on a cleaned and polished silicon wafer, thus passivating the surface.

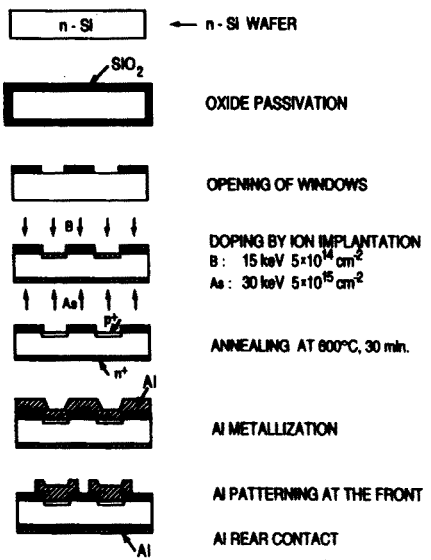

Fig. 2. Outline of the steps in fabricating planar, ion-implanted silicon detectors.

Photolithographic techniques are used to open windows through which ion implantation produces the junction layer on the front face and an ohmic layer on the rear face. Following annealing, aluminization is carried out, allowing contacts to the individual diodes to be made. Rather complex geometries can readily be fabricated, with segmentations in the micron regime. The major challenge is in making connections to the individual channels and

also providing the very large number of electronics channels required to fully exploit these very high segmentations. These needs have, in turn, spurred the development of sophisticated, custom-built, micro-circuit preamplifiers, ADCs and logic units for use with high segmentation silicon strip detectors.

The most common design of such detectors takes the form of parallel strips along the junction face of the detector. Two-dimensional information is then obtained by stacking detectors with the strips at right angles to each other. Two-dimensional detectors have also been developed in which strips are formed in orthogonal directions on both the junction and ohmic faces, thus forming a quasi-pixel detector. This type of detector is, however, still subject to the well-known ambiguities in x and y coordinates which occur for multiple-hit events. True pixel or pad detectors are now also being developed. The major challenge is to make electrical contact with each pixel and to provide the requisite number of electronics channels.

Until recently, detectors of this type had not been widely used in low-energy nuclear physics, perhaps because of the relatively high cost of a custom detector and electronics design. However, as more types of detector have been fabricated and as low-energy nuclear physics experiments have become more complex, their use has become more common. In the following sections two such applications are described. Other important applications, which are not described here, involve implantation of heavy nuclei into double-sided strip detectors and searching for their subsequent, spatially correlated radioactive decay. With this method, the heaviest known elements have been identified as well as many examples of new proton radioactivities.

3. Search for exotic alpha chain states in ^{24}Mg

Several calculations [4, 5] have predicted that exotic configurations consisting of linear chains of alpha particles may be quasi-stable in light nuclei. One example is shown in Fig. 3, where the result of a Nilsson-Strutinsky calculation of the potential-energy surface of ^{24}Mg is shown in comparison with density contours for quasi-stable configurations found in a cluster model calculation. In addition to the ground-state minimum with modest prolate deformation, several extremely deformed minima are observed, including one corresponding to a linear chain of six alpha particles. The experimental identification of this configuration presents quite a challenge as its expected excitation energy is such that it is unbound for decay into its constituent alpha particles. It is, however, this decay mode which provides the best opportunity for identifying the chain state. The structure of the chain suggests that the most likely decay mode is for the six-alpha chain to split in to two three-alpha chains, corresponding to the well-known excited

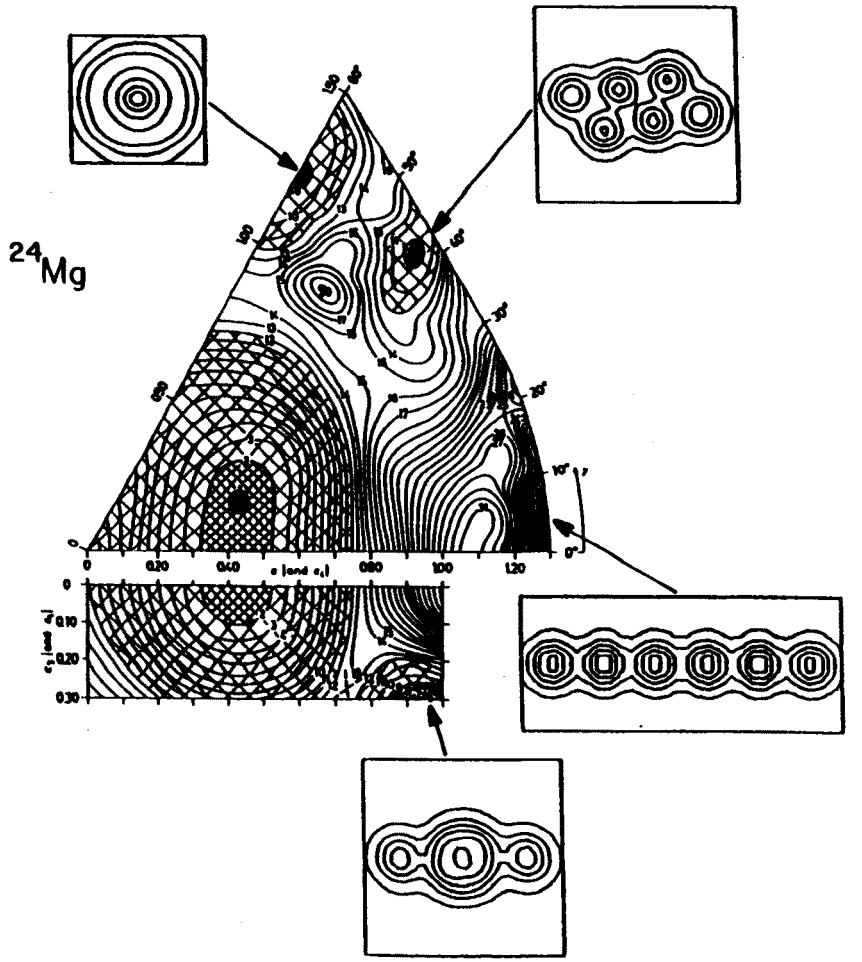

Fig. 3. Comparison between the potential energy surface of ^{24}Mg from the deformed shell model and density contours from a multi-center cluster model.

0^+ state at 7.65 MeV in ^{12}C. This state in ^{12}C subsequently itself decays to ^{8}Be — the two-alpha chain — plus alpha, and the ^{8}Be then also decays to two alpha particles. Thus, the six alpha particles resulting from the decay of the ^{24}Mg state appear in a kinematically highly correlated fashion due to the sequential nature of the decay process outlined above. The relatively low energies involved in the ^{12}C and ^{8}Be decays means that the resulting alpha particles are also spatially correlated, being confined to cones with opening angles of only a few degrees. This allows their detection with high probability in a detector with only relatively modest dimensions.

The six-alpha final state populated via the $^{12}C + ^{12}C$ entrance channel was studied [6] using double-sided strip detectors each of which consisted of a 5×5 cm^2 Si wafer with 16 strips each 3 mm wide on the front and back faces. Two of these detectors were used, one on each side of the beam axis at a distance of 15 cm, thus giving 512 quasi-pixels each subtending an angle of approximately 1 degree. In subsequent measurements, up to six such detectors have been used. The detectors were read out using custom--built 16 channel preamplifier modules [7] each of which provided energy and timing signals for input into charge integrating ADC's and constant fraction discriminators respectively. The overall resolution was 25 keV for 6 MeV alpha particles and the time resolution was 500 ps. The position ambiguities resulting from multi-hit events were resolved by requiring that the energies obtained from the front and back strips of the detector match for each hit, thus enabling in most cases a unique association of the x and y coordinates.

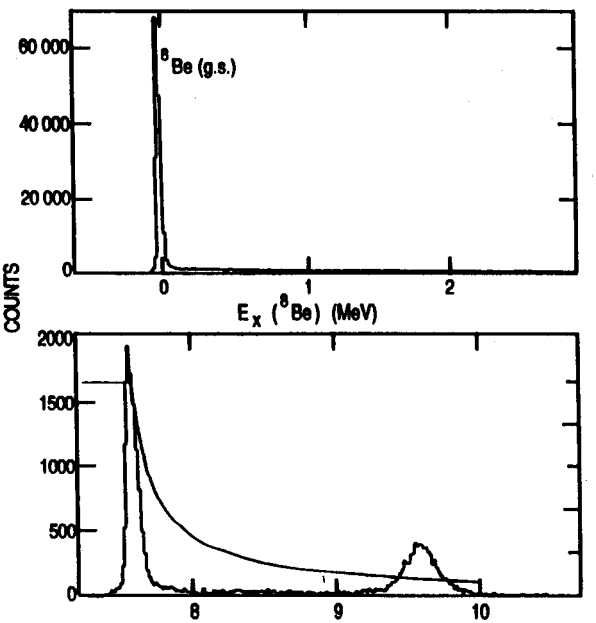

Fig. 4. Excitation energy spectra for 8Be and ^{12}C from two and three alpha particles. The solid curve in the lower portion is the calculated efficiency.

Examples of reconstructed excitation energy spectra from two and three alpha-particles are shown in Fig. 4, clearly showing the ground state of ^{8}Be and the 7.65 MeV 0^+ and 9.64 MeV 3^- states in ^{12}C. Also shown on the lower portion of the figure, is the calculated efficiency curve for three-alpha

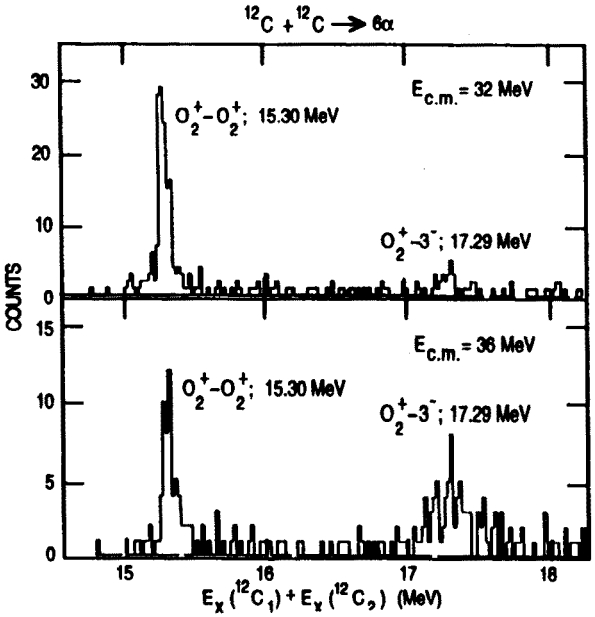

Fig. 5. Total excitation spectrum for events in which six alpha particles are detected.

events. The decline in efficiency with increasing excitation energy results from the increase in the opening angle of the three alphas with excitation energy and the size of this cone relative to the angular acceptance of the detector. Figure 5 shows the reconstructed Q-value spectrum for six-alpha events, measured at two bombarding energies. The peak at $Q = -15.30$ MeV corresponds to both ^{12}C nuclei in the excited 0^+ state, the expected signature of the decay of the chain configuration in ^{24}Mg.

An excitation function for the $(0^+, 0^+)$ channel is shown in Fig. 6 which reveals a striking, strong broad structure centered at a center-of-mass bombarding energy of 32.5 MeV, corresponding to an excitation energy of 46.4 MeV in ^{24}Mg. The width of the observed structure (5 MeV) is too large for this to represent a single isolated resonance as the decay time implied by this width is less than the rotation time of the dinuclear $^{12}C + ^{12}C$ system. This observation is underlined by angular distributions [8] measured over the structure which, although apparently dominated by a few angular momenta in the region of 12–14$\hbar$, are quite complex in structure and do not correspond to a single Legendre polynomial as would be expected for an isolated resonance. Interestingly, the excitation energy and angular momenta suggested by these data place the observed structure very close to the expected location of the predicted alpha-chain state as is shown in Fig. 7.

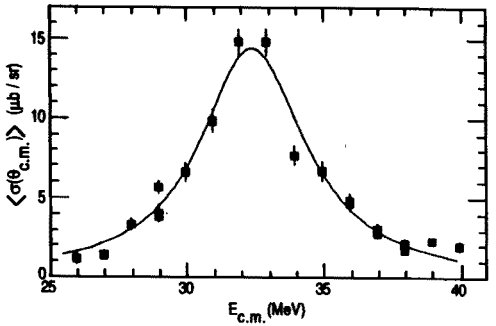

Fig. 6. Cross-section for the double 0^+ excitation shown as a function of bombarding energy.

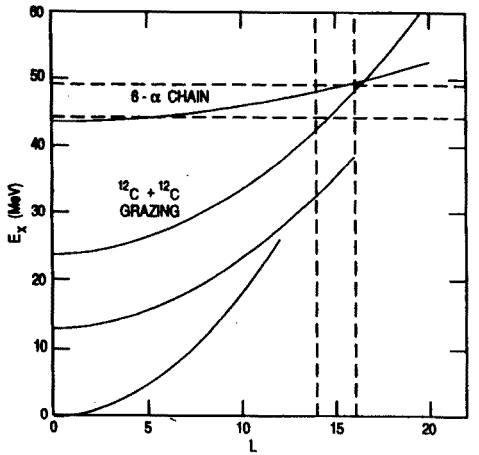

Fig. 7. Plot of excitation energy versus spin for ^{24}Mg showing the predicted location of the six-alpha chain band. The location of the observed structure is indicated by the dashed lines.

Other features of the angular distributions, such as a pronounced maximum at 90 degrees which implies a constructive interference of several even partial waves, also suggest that the measured structure may correspond to a degenerate rotational cluster band [9] similar to the alpha-chain band in ^{24}Mg.

4. Positron-electron pairs from heavy ion collisions

Narrow peaks have been observed [10] in the energy spectra of positrons and sum-energy spectra of positron-electron pairs produced in collisions of

very heavy ions at near-barrier energies. To date there is no satisfactory explanation of the origins of these lines although many differing models have been proposed. A second-generation experiment, designed to study these phenomena has been designed and constructed and is called APEX (ATLAS Positron EXperiment). The experiment is now complete and the first data are being produced.

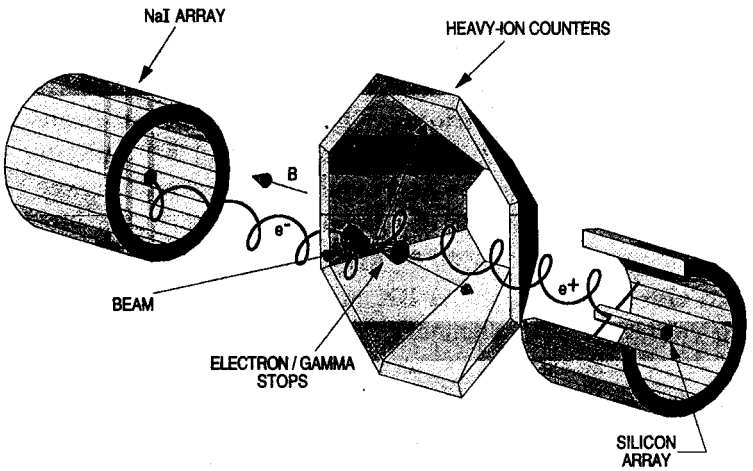

Fig. 8. Conceptual drawing of APEX showing the major components.

The conceptual design of APEX is shown in Fig. 8, which displays the main components of the apparatus. Briefly, the apparatus consists of a large solenoid with a field of 300 Gauss, mounted transverse to the beam direction. A rotating target wheel at the center of the device is designed to allow the use of targets such as U and Th with minimum deterioration due to heating and to reduce the effects of sputtering and thus allow intense beams of the heaviest ions such as U. Scattered ions and the recoiling target nuclei are detected in an array of twenty-four position-sensitive gas counters which allow the reconstruction of the kinematics of the heavy-ion scattering associated with the positron production. Situated close to the target on either side, on the solenoid axis, are two cone-shaped pieces of heavymet, coated with low-Z material to suppress positron production on their surface. These serve the dual purpose of shielding the annihilation detectors from gamma and X-rays produced at the target as well as providing a geometrical suppression of the intense flux of low-energy electrons. The geometry of these "electron/gamma stops" is such that they intercept the trajectories of all electrons and positrons with energies less than approximately 120 keV. Leptons which pass into the outer regions of the field, travel in helical trajectories until they strike one of the two silicon detector arrays, positioned

on the magnetic axis of the solenoid. These detectors provide information on the energy, time of arrival and position for the positrons and electrons which strike them. Positron identification is accomplished by detection of the characteristic annihilation radiation in two twenty-four element arrays of position-sensitive NaI arrays which also provide the basic trigger for the experiment. Information provided by the NaI arrays is used to calculate the source of the back-to-back annihilation photons and thus the position of the positron annihilation on the silicon array.

The apparatus was completed in summer 1993 and the measurements of positron and positron-electron coincidences have been made under a number of different experimental conditions. The acceptance and response of the apparatus has been studied both with sources and by studying different aspects of the in beam data. The first results have been presented elsewhere [11, 12] and will therefore not be discussed here. Of primary interest in the context of this paper is the silicon array, which is discussed in detail below.

The two silicon arrays in APEX are key components of the experiment. Each consists of 216 elements, 3 cm long by 0.5 cm wide, arranged on the surface of a hexagonal structure, 36 cm long and approximately 3 cm in diameter. The basic detector modules are trapezoidal in shape and each contain three independent active elements. Six of these modules are mounted on hexagonal rings, twelve of which are stacked like the roofs of a chinese pagoda. Readout is accomplished using flexible printed circuit board strip lines which carry signals, bias and ground connections to feedthrough boards which run through the vacuum wall. Multilayer boards which contain the preamplifiers are mounted off these feedthroughs on the immediate outside of the vacuum flange.

The physics requirements of the experiment demand that the silicon detectors provide good energy and timing resolution ($<$10 keV and $<$2 ns) as well as good detection efficiency for electrons and positrons up to 1 MeV in energy. The latter requirement implies that the silicon be at least 1 mm in thickness. The number of detectors and the complex geometry of the arrays suggested that ion-implanted surface passivated diodes were the only practical choice. However, at that time such devices were only made in thicknesses up to 500 microns. The major technical issue in the fabrication of thicker devices of this type relates to the higher voltages required to fully deplete the thicker wafers and the prevention of breakdown due to the consequently higher surface fields. In part this can be helped by the use of higher resistivity silicon, but this material is not readily available in quantity and is also subject to a reduction in resistivity due to contamination in processing. These problems were circumvented by a detector design [13, 14] incorporating guard ring structures in the region between the active areas and the cut edges of the wafer. The guard ring structures not only result in

reduced field strength near the cut edges of the wafers but also shunt any surface currents away from the active areas. A drawing of the three-element APEX detector is shown in Fig. 9. Room temperature leakage currents as low as a few nanoamps per active strip were obtained.

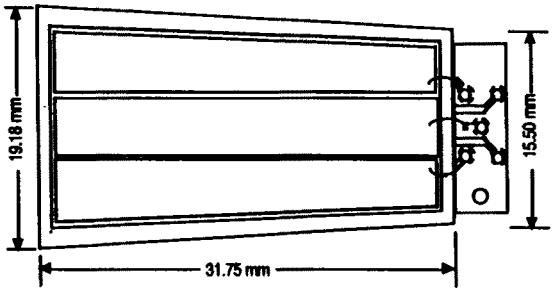

Fig. 9. The three-element APEX silicon detector. The detector is mounted on a ceramic substrate.

A number of different evaluations of these detectors was carried out, ranging from simple applied-voltage, current measurements to energy and timing resolution measurements with a variety of sources. To improve both the energy and timing resolutions, it was found advantageous to cool the detectors resulting in reduced leakage currents and improved charge collection due to the increased carrier mobilities at low temperatures. The results of these tests and the effects of cooling are shown in Fig. 10 where the data were taken using the preamplifier developed specifically for APEX. In the actual APEX apparatus, the cooling of the silicon arrays is accomplished using boil-off gas from liquid nitrogen which flows over the silicon detectors at a pressure of 100 torr. The separation of the cooling gas from the chamber vacuum is by a thin, tubular shroud of aluminized Kapton which surrounds the arrays.

An example of the performance of the arrays is shown in Fig. 11 where the energy spectrum obtained from a ^{113}Sn source placed at the target position is shown. This spectrum represents a sum of the spectra of 216 elements of one of the arrays. The overall resolution obtained is 11 keV as is demonstrated by the observed K and L conversion lines which are separated by 24 keV.

For positron-electron pairs, ^{90}Y provides a convenient source which also gives an intense background of electrons similar to that in the in-beam situation. ^{90}Y decays largely via e^- emission to the ground state of ^{90}Zr but has a weak (0.011%) branch to the 1761 keV 0^+ state, which subsequently decays by pair emission to the ground state. The sum energy of the pair is 739 keV. Figure 12 shows the sum-energy spectrum of positron-electron pairs from such a measurement. The sum-energy peak corresponding to the

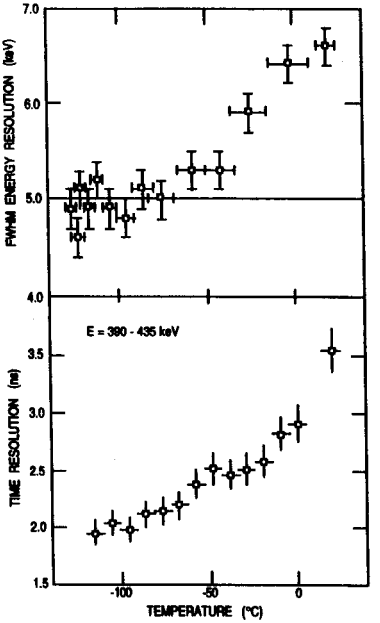

Fig. 10. Energy and time resolution of APEX detectors as a function of temperature. For details see Ref. [14].

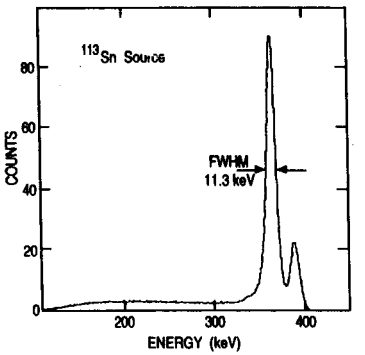

Fig. 11. Energy spectrum of ^{113}Sn measured in one of the APEX silicon arrays.

0^+ decay is observed with a width of approximately 27 keV. These data were taken with a 30 mCi source which gives a total electron count rate of 10^6, comparable to the number produced in-beam within the energy acceptance of APEX, the ability of the array to handle these high count rates of course comes from the high degree of segmentation.

Thus, it has been possible to construct a high resolution detector for electrons and positrons in the energy range up to 1 MeV which is able to identify the relatively rare positrons in the presence of intense backgrounds

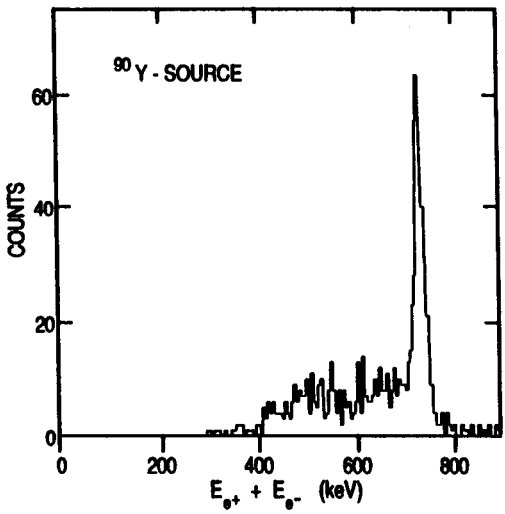

Fig. 12. Sum-energy spectrum of identified positrons and electrons from ^{90}Y decays.

of photons and electrons. The versatility of ion-implantation technology has allowed the construction of a geometrically complicated array optimized for the needs of the experiment rather than constrained by the detectors themselves.

5. Future possibilities

From the preceding sections we have seen the versatility and power of the new types of detectors which can be fabricated from ion-implanted silicon, and how these can have major impact on low-energy nuclear physics research. There are, however, some issues of cost and complexity which need to be addressed.

First, the major cost of a custom designed ion-implanted detector lies in the masks used in the photo-lithographic processes which represent a significant, but non-recurring, contribution to the total cost of any new design. On the other hand, the incremental cost of additional detectors is quite low. Thus, unless there are already existing designs which can be used, any new application will require significant development and must also be of sufficient size or importance to merit the investment.

Second, the large number of channels that result from the use of large numbers of highly segmented detectors places severe stress on the electronics, both in making connections to the small detector elements and in the large costs associated with many channels. It is interesting to note that the electronics costs of the two applications discussed above, which use custom built although conventional circuits, work out to be almost identical

on a per channel basis, $\sim$ \$ 800 each from preamplifier to digitization. In high-energy physics applications, this problem has been solved through the development of custom-designed integrated circuits containing both analog and digital circuits for processing of the signals. As is also the case for the detectors, however, there are also large non-recurrent expenses associated with the circuit design which can only be cost effective if large numbers are to be produced — the ultimate cost per channel being only tens of dollars. Application of these ideas in low-energy physics also raises the issues of the specific needs of these experiments which, in general, may be harder to fulfill than the typical high-energy experiment for which a hit pattern or only limited dynamic range may be sufficient.

Nevertheless, there are areas of low-energy nuclear physics where such effort might be well justified. In particular, a particle "ball" built to operate in conjunction with one of the new generation of 4π gamma-ray arrays would present many new and exciting physics opportunities. Such an array would require significant development, particularly in the area of electronics such that the much larger pulse heights from low-energy particles can be read out with sufficient resolution and also high-resolution time-of-flight measurements carried out for particle identification purposes. Rough estimates of the cost of a 10 cm radius sphere of silicon with 2×2 mm^2 quasi-pixels obtained from double-sided strip detectors, including electronics, are of order US \$ 1M, which still represents a relatively small fraction of the total cost of the gamma arrays themselves. Also, such a device would be extremely powerful in stand-alone mode and would allow, for example, extensions of the kind of studies described in Section 3 as well as other new types of experiments.

Collaboration with Alan Wuosmaa, Tom Happ, Martin Freer, Irshad Ahmad and Lars Evensen in many aspects of the work described here is gratefully acknowledged. The detectors used in the experiments described here were supplied by Micron Semiconductor, England and SINTEF, Norway. Work at Argonne National Laboratory is supported by U.S. DOE under contract number W-31-109-ENG-38.

REFERENCES

[1] For reviews see: G. Hall, *Rep. Prog. Phys.* **57**, 481 (1994); J.M. McKenzie, *Nucl. Instr. Meth.* **162**, 49 (1979); G.T. Ewan, *Nucl. Instr. Meth.* **162**, 75 (1979).
[2] D.A. Bromley, J.A. Kuehner, E. Almqvist, *Phys. Rev. Lett.* **4**, 365 (1960).
[3] J. Kemmer, *Nucl. Instr. Meth.* **226**, 89 (1984).
[4] G. Leander, S.E. Larsson, *Nucl. Phys.* **A239**, 93 (1975).

[5] S. Marsh, W.D.M. Rae, *Phys. Lett.* **108B**, 185 (1986).
[6] A.H. Wuosmaa *et al.*, *Phys. Rev. Lett.* **68**, 1295 (1992).
[7] A.H. Wuosmaa *et al.*, *Nucl. Instr. Meth.* **A345**, 482 (1994).
[8] A.H. Wuosmaa *et al.*, *Phys. Rev.* **C** , in press.
[9] W.D.M. Rae, A.C. Merchant, B. Buck, *Phys. Rev. Lett.* **69**, 3709 (1992).
[10] J. Schweppe *et al.*, *Phys. Rev. Lett.* **51**, 2261 (1983); M. Clemente *et al.*, *Phys. Lett.* **137B**, 41 (1984); H. Tsertos *et al.*, *Phys. Lett.* **162B**, 273 (1985); T. Cowan *et al.*, *Phys. Rev. Lett.* **54**, 1761 (1985); T. Cowan *et al.*, *Phys. Rev. Lett.* **56**, 444 (1986); W. Koenig *et al.*, *Z. Phys.* **A328**, 129 (1987); H. Tsertos *et al.*, *Z. Phys.* **A328**, 499 (1987); E. Berderman *et al.*, *Nucl. Phys.* **A488**, 683c (1988); W. Koenig *et al.*, *Phys. Lett.* **218B**, 12 (1989); P. Salabura *et al.*, *Phys. Lett.* **245B**, 153 (1990); H. Tsertos *et al.*, *Z. Phys.* **A342**, 79 (1992); I. Koenig *et al.*, *Z. Phys.* **A346**, 153 (1993).
[11] I. Ahmad *et al.*, Proceedings of Fifth International Conference on Nucleus Nucleus Collisions, Taormina, Sicily, June 1994, *Nucl. Phys.*, in press.
[12] I. Ahmad *et al.*, Proceedings of Conference on Physics from Large Gamma-ray Arrays, Berkeley, CA, USA, August 1994, in press.
[13] I. Ahmad *et al.*, *Nucl. Instr. Meth.* **A299**, 201 (1990).
[14] L. Evensen *et al.*, *Nucl. Instr. Meth.* **A326**, 136 (1993).